**Fifty Years of Ion and Neutral Thermochemistry by Mass Spectrometry**

P. B. Armentrout

Department of Chemistry, University of Utah, 315 S. 1400 E, Salt Lake City, UT 84108, USA

**Abstract**

Originating with the appearance potentials for "positive rays", the ability of mass spectrometry to obtain quantitative information about the energetics of both ions and neutrals has evolved dramatically. About 50 years ago, many of the techniques that are now common place were first implemented, the interim has seen significant advances in both instrumentation and analysis tools. In this review, a short historical perspective of mass spectrometric approaches to ion and neutral thermochemistry is provided. Included are determinations of ionization and appearance energies, electron affinities, and dissociation energies. The latter are explored via techniques utilizing metastable decomposition, visible and vuv photodissociation, infrared photodissociation, collision-induced dissociation, and electron-induced dissociations, as well as applications of equilibrium methods and association processes. Although many of these techniques focus on ion thermochemistry, the ability to measure the thermodynamics of neutrals via mass spectrometric approaches is also highlighted.

*keywords: appearance energy, association, collision-induced dissociation, electron affinity, equilibrium, ionization energy, photodissociation*



UU IR Author Manuscript

**Introduction**

Early experiments found that the appearance of "positive rays" was strongly influenced by the electric potential used to accelerate the electrons forming them. (Positive rays were ionized atoms and molecules [1], as first identified by Goldstein in 1886 [2]. Wien found that they were positively charged and much more massive than electrons, as demonstrated by deflection in a magnetic field [3].) This observation leads naturally to the realization that quantitative thermodynamic information might be obtained from mass spectrometric experiments. Indeed, early measurements determined that the minimum potential needed to create positive rays (by ionizing the gas) varied with the gas identity. This minimum potential equals the ionization energy, although the earliest such experiments generally did not include identification of the mass of the species. When mass characterization was included, the cationic species formed by ionization of molecular species near the threshold was generally found to be the intact molecule. At higher accelerating potentials, these molecular species were found to fragment. Measurements of such appearance energies rapidly expanded the thermochemical database for ions. F. H. Field and J. L. Franklin published one of the first compilations of such thermodynamic information in 1957 [4]. Subsequent versions include "Gas-phase Ion and Neutral Thermochemistry" (or "GIANT Tables") [5], proton affinity evaluations [6], and now the NIST Webbook [7 2014) #2844 2014), (retrieved March 6, 2014), (retrieved March 6, 2014) #2844], which contains regularly updated and evaluated thermodynamic information on ions and neutrals. Since these early days, increasingly sophisticated tools, many of which are covered thoroughly in an excellent review elsewhere [8], have been employed to examine the thermodynamics of ions and their neutrals. Here, we briefly recount historical aspects of the development of many of these experimental methods over the past 50 years or so.

Any account of ion thermochemistry must include the conventions for treating the enthalpy of the electron. Most thermodynamicists (including this author) use the "electron convention", where the enthalpy and free energy of formation of the electron are zero at all temperatures, as for any element. This convention allows the enthalpies and free energies of

UU IR Author Manuscript

formation for all substances to change little with temperature. (It is also useful to recall that enthalpies and free energies are equal at zero K, but deviate somewhat at higher temperatures because of the contribution of entropy.) Many mass spectrometrists prefer the "ion convention", where the enthalpy of formation of the electron is assigned to equal its heat capacity. Generally, the heat capacity of the electron is assumed to follow Boltzmann statistics (5RT/2 or 6.197 kJ/mol at 298 K. A more correct treatment uses Fermi-Dirac statistics (3.145 kJ/mol at 298 K) [9,10]. Because the enthalpies of formation of ions at nonzero temperatures vary with the convention adopted, this must be specified in careful work.

**Ionization and Appearance Energies**

As noted in the introduction, ionization energies were the first thermodynamic data obtained concerning ions. The earliest determinations generally involved electron ionization, such that the minimum accelerating potential needed to induce ionization of a gas by electrons was measured. Hence, "ionization potential" was the term used originally, but as other means (e.g., photons) can be used to ionize gases, the preferred term is ionization energy (IE). The process involved is shown in reaction (1), where the enthalpy of reaction simply equals the IE.

$$AB + e^-(h\nu) \rightarrow AB^+ + 2\,e^-(e^-) \qquad \Delta_r H = IE \qquad (1)$$

(This reaction also makes clear why ion enthalpies of formation depend on the convention used for the electron enthalpy.) The threshold laws for electron and photon ionization differ, as shown by Wigner [11]. For photoionization, the onset is a step function, whereas the probability of electron ionization increases linearly with electron energy exceeding the threshold. Because of the sharp rise associated with photoionization, more precise thresholds can generally be obtained, as demonstrated nicely for atomic species. Photoionization of molecular species was not accomplished until the middle of the 20$^{th}$ century and originally did not include mass selection. For example, the photoionization of NO showed steps in the photoionization yield that corresponded to the vibrational levels of $NO^+$ [12]. In this favorable case, the low IE of NO meant that ionization of other species present did not occur, hence no mass resolution was

UU IR Author Manuscript

needed. For electron ionization, which was easier to implement experimentally, early developments included using electron monochromators to narrow the width of the electron energy distributions (to 50 – 70 meV) that lead to lower resolution in the IE onset. Less rigorous "quasi-monoenergetic" methods [13], such as retarding potential difference and energy distribution difference methods, were also developed.

When mass spectrometers were added to the instruments used to measure ion yields, the formation of molecular fragments (rather than the intact molecular ion) could now be observed. Using the same approaches as for IE measurements, appearance energies (AEs, originally "appearance potentials") of fragment ions could be determined. Here the enthalpy of reaction is that shown in reaction (2).

$$AB + e^- (h\nu) \rightarrow A^+ + B + 2\,e^- (e^-) \qquad \Delta_r H = AE \qquad (2)$$

In 1958, photoionization sources were first coupled with mass selection [14]. A couple of years later, the use of a He discharge lamp as a monochromatic light source was employed for vuv photoelectron spectroscopy [15,16] in which the kinetic energies of the ejected electrons were first measured. The year 1967 saw the first measurement of threshold photoelectrons [17], as well as the first coincidence measurements of photoelectrons and photoions (PEPICO) [18]. Several threshold types of measurements have enhanced the resolution of such studies even further [19] and include threshold photoelectron spectroscopy (TPES), which is also known as ZEKE spectroscopy (zero kinetic energy electrons) [20,21], pulsed field ionization (PFI) [22], and threshold PEPICO (TPEPICO) experiments. An example of the dramatic improvement in resolution (and hence information) is shown in Figure 1 for the ionization of benzene [23]. This compares results from regular photoelectron spectroscopy (PES) and photoionization studies (showing the vibrational steps alluded to above for NO) with PFI results. Comparison of the top and bottom spectra show an enhancement in the resolution of about an order of magnitude (linewidths of ~10 and ~1 meV, respectively). (Some of the resolution enhancement is also attributable to the use of a supersonic expansion. The direct effects of this are better quantified for the case of benzene by Long et al. [24], who found linewidths in their photoelectron spectra

UU IR Author Manuscript

of 6 – 10 meV for an effusive source and 3 – 5 meV for a supersonic expansion.) More recently, free electron (synchrotron) light sources have greatly expanded the range of systems studied by extending the photon range and intensity [19,25,26].

The methods described above provide many of the available IE and AE values, but additional approaches are valuable in unusual circumstances. Notably, this includes cases where Franck-Condon (FC) factors make it difficult to observe the adiabatic IE. Classic examples include $NO_2$ and $CH_4$, which greatly distort upon ionization. In such cases, accurate IEs (although less precise than spectroscopic) can be obtained using charge transfer reactions, which can be conducted as equilibrium, bracketing, or threshold measurements [27,28], see below. The $NO_2$ case is exemplary. Here, the bent $NO_2$ molecule distorts to linearity upon ionization ($NO_2^+$ is isoelectronic with $CO_2$). Hence, PES exhibits no intensity at the adiabatic IE and adiabatic IE values ranging from about 9.8 to 12.3 eV had been reported, with a couple of spectroscopic results indicating a value near 9.6 eV but a chemical reaction indicating a lower limit of 9.685 eV (as reviewed in [28]). At the time, the most definitive measurement in the literature had been performed by Grant and coworkers who used multiple photon processes to overcome the FC restrictions, and obtain a very high precision IE [29]. Here, two photons (of different color) were used to resonantly excite $NO_2$ to a linear Rydberg state, which was then photoionized with a third photon. Their onset was 9.586 ± 0.002 eV, although it was possible that this value could have corresponded to an excited vibrational state of $NO_2^+$, which would have shifted the true adiabatic IE down by 0.076 eV. In our laboratory, we examined the kinetic energy dependence of several charge transfer reactions with both $NO_2$ and $NO_2^+$. The most definitive result was the observation that charge transfer with $Zn^+$ was endothermic by 0.21 ± 0.03 eV, indicating IE($NO_2$) = 9.60 ± 0.03 eV [28,30]. In this case, the FC restrictions are overcome because nuclear motion is an intrinsic part of this endothermic charge transfer reaction, hence relaxation of the structure of the $NO_2$ upon ionization occurs naturally during the course of the reaction. The agreement between our result and the very precise value from Grant and coworkers verifies that this is the correct adiabatic IE.

UU IR Author Manuscript

**Electron Affinities**

The first measurements of electron affinities (EAs) were attempted using electron attachment at hot filaments and from dissociative attachment experiments, but the reliability of such measurements is questionable. About 50 years ago, the first accurate electron affinity was determined using photodetachment (PD) spectroscopy with a broadband light source and filters [31]. Modern applications that utilize tunable laser light sources provide much more precision [32], as illustrated in Figure 2. Here, the early PD measurement of EA(O) using broadband light [33] yields a value of 1.465 ± 0.005 eV, but this clearly relies on accurately knowing the threshold law to extrapolate the data properly. The modern PD spectrum using tunable laser light [34] provides a spectrum ranging from 1.432 to 1.494 eV, a very small fraction of the former spectrum. Note that the shape of the various steps observed in the latter spectrum match that in the older measurement. These features correspond to transitions between the fine structure levels of $O^-$ ($^2P_{3/2,1/2}$) and O ($^3P_{2,1,0}$). The step (labeled 3) corresponding to the adiabatic EA occurs at 1.461110 ± 0.000001 eV.

Another precise method of determining anionic thermochemistry is the measurement of ion-pair production in ionization experiments. Although of limited applicability (about 50 small molecules) [8], reaction (3) yielding both positive and negative ions is observed.

$$AB + h\nu\,(e^-) \rightarrow A^+ + B^- \,(+ e^-) \qquad \Delta_r H = D(AB) + IE(A) - EA(B) \qquad (3)$$

Here, the reaction enthalpy simply equals the photon (or electron) energy at threshold. As with similar IE measurements, the development of threshold ion-pair production spectroscopy (TIPPS) [35], which utilizes technology similar to PFI, has greatly enhanced the precision of this technique. For example, the 0 K bond dissociation energy of $H^{35}Cl$ taken from information in the JANAF Tables is 4.4336 ± 0.0022 eV [36], whereas the TIPPS value is 4.4322 ± 0.0001 eV [37].

Although the precision of photodetachment spectroscopy cannot be achieved easily by other methods, its applicability to measuring EAs for a wide range of species is more limited. A

UU IR Author Manuscript

more general technique is photoelectron spectroscopy (PES) of anions using fixed frequency light sources followed by measurement of the electron kinetic energy, which limits the precision to a few meV. First applied just less than 50 years ago (to the unlikely case of $He^-$) [38], it was later extended to molecular species [39]. Enhanced precision can again be achieved using the ZEKE approach [40,41], and the addition of imaging techniques in the slow electron velocity-map imaging (SEVI) method combines that precision with more sensitivity [42]. For example, Wang and coworkers have recently measured EA($Au_2^-$) = 1.9393 ± 0.0006 eV [43], in good agreement with a ZEKE result of 1.9400 ± 0.0005 eV [44] and the more conventional PES value of 1.938 ± 0.007 eV [45].

**Dissociation Energies**

Once IE and AE measurements had been established, it was quickly realized that the difference between these onsets yielded the bond dissociation energy (BDE) for the $AB^+$ ion, the enthalpy of reaction (4).

$$AB^+ \rightarrow A^+ + B \qquad \Delta_r H = D(A^+\text{–}B) = AE - IE \qquad (4)$$

A host of bond energies from such measurements were tabulated, but it became apparent that the accuracy of this thermochemistry was more complicated than the simple determinations of the onsets. Specifically, the fragmentation reaction (4) might have a barrier in excess of its endothermicity. More generally, AEs can be influenced by the internal energy of AB, which lowers the onset measured, and by the kinetics of dissociation [46] and competition between parallel dissociation channels [47], which delay the onsets by amounts that depend on the details of the instruments used. Such subtleties can be evaluated by including detailed analysis of the kinetics for fragmentation along with the energy distributions involved in the ionization and fragmentation steps. An example PEPICO study is shown in Figure 3 for $Co(CO)_3NO$ ionization followed by four subsequent dissociations [48]. Precisions in the cationic bond energies derived are about 0.02 eV. In this system, the data were also combined with the BDE for $Co^+$–CO from threshold collision-induced dissociation (TCID) studies [49] (see below), which then allows the

absolute energy scale to be fixed to the $Co^+$ + 3 CO + NO asymptotic energy. From this, enthalpies of formation of the neutral precursor and various cationic fragments could all be established.

In addition to these methods of determining ionic BDEs, more direct means of interrogating such fragmentations can be applied. Addition of the energy needed for fragmentation can be supplied by the intrinsic energy content in the ions (metastable dissociation), photons, collisions with gases, or by electrons, as outlined in the following sections.

**Metastable Dissociation**

The spontaneous decomposition of metastable ions can be used to acquire thermodynamic information by measurement of the kinetic energy release distribution of the fragments (KERD), typically in an electrostatic analyzer. Such distributions can be either statistical, as is typical for a loose transition state (TS) associated with no reverse activation barrier to dissociation, or nonstatistical for passage over a tight TS located at a barrier [50]. Although accurate identification of the maximum kinetic energy can lead to the measurement of the energy of the bond being broken, it is much more reliable to model the entire distribution, which is feasible for the case of the loose TS. For instance, Carpenter et al. examined the formation of $M^+(CO)$ from $M^+$(acetone) for $M^+$ = Fe, Co, and Ni [51]. The $D(M^+–CO)$ values obtained, 1.38, 1.70, and 1.67 ± 0.13 eV, respectively, compare well to values obtained from TCID measurements, 1.36 ± 0.08, 1.80 ± 0.07, and 1.81 ± 0.11 eV, respectively [49,52,53].

Metastable dissociation can also be used to determine relative binding energies by utilizing the Cooks' kinetic method approach [54]. As originally conceived, metastable dissociation of proton-bound dimers, $A–H^+–B$, were studied (although the concept is straightforwardly extended to dimers of any $M^{+/-}$ cation or anion and can be augmented by collision-induced dissociation as well). In all cases, the relative magnitudes of the products, $MA^{+/-}$ and $MB^{+/-}$, should reflect the relative ion affinities of A and B presuming that the

UU IR Author Manuscript

dissociations are in some sort of quasi-equilibrium at the "effective temperature" of the excited dimer complex. If the ion affinity of either A or B is known, then the other can be estimated. Accuracy is greatly enhanced by studying a series of knowns relative to a single unknown because this allows interpolation of the unknown ion affinity. In its simplest incarnation, a variety of assumptions are needed to extract meaningful thermodynamic values, and extended treatments of various sorts have been applied with reasonable success [55,56]. The validity of the kinetic method approach has been commented on extensively [57-59]. This method is used often because it can be applied using commercial instruments, but the accuracy of this approach remains less refined than others discussed below.

**Visible and vuv Photodissociation**

For thermodynamic work, the most informative photodissociation experiments are generally conducted under single photon conditions, i.e., using visible or ultraviolet light to break the bond of interest. Many of the earliest studies involved measuring the onset for photodissociation as a function of photon energy, which requires that there be an absorbing state available at the threshold [60]. Hence, these studies often focused on species containing metals because the higher electronic state density of the metal enhances that probability. In cases where the photon energy is absorbed at energies above the threshold, accurate thermochemistry can still be obtained by measuring the kinetic energy of one of the photodissociation fragments in photofragment translational spectroscopy (PTS), first introduced in 1985 [61]. Accurate information requires knowledge of the internal energy of the fragments or determination of the onset of the kinetic energy distribution. For instance, the kinetic energy distribution of the $O^-$ product formed by photodissociation of $N_2O_2^-$ at 570 nm (2.175 eV) is shown in Figure 4 [62]. The peaks in this spectrum can be associated with excitation of the bend in the $N_2O$ neutral fragment, with the highest energy peak assigned to the ground vibrational level with rotational excitation contributing to its width and position. The onset of this peak at 0.78 ± 0.03 eV therefore suggests that $D_0(O^-\text{-}N_2O)$ = 1.40 ± 0.03 eV (a value that assumes negligible internal

excitation of the supersonically cooled $N_2O_2^-$ reactant). Notably the kinetic energy onsets for the $O^-$ product at 500 and 520 nm are not easily observed nor are they for the competing $NO^-$ + NO channel at all three wavelengths. Likewise PTS studies of $O_4^-$ were not used to determine the $O_2^-$–$O_2$ bond energy (previously well-characterized by PHPMS studies [63], see below) because the parent ion internal energy could not be characterized [64].

First developed in 1987, time-resolved photodissociation (TRPD) irradiates trapped ions while monitoring their intensity [65]. The dissociation kinetics are then modeled using statistical unimolecular decay theory to extract thermodynamic data. For example, dissociation of *p*-iodotoluene has been studied at low photon energies using TRPD (ions at 375 K) and at higher photon energies using PEPICO (ions at 300 K), as shown in Figure 5 [66]. By combining these measurements, the kinetic model is highly restricted such that an enthalpy and entropy of dissociation are determined as 1.9 eV and 17 J/K mol, respectively. In addition, because the dissociation rate at the lowest photon energy (1.97 eV) is so slow, infrared radiative relaxation becomes very important, indeed the authors estimated that "at this wavelength only one-tenth of the photoexcited ions succeed in dissociating before relaxing by ir emission."

**Infrared Photodissociation**

Observations like this soon led to the realization that such ions can be in thermal equilibrium with ambient blackbody radiation [67]. Perhaps less obviously, this radiation can lead to dissociation, as originally demonstrated in a technique called zero-pressure thermal radiatively induced dissociation (ZTRID) [68,69]. Originally applied to relatively small molecules, it was realized that because larger molecules dissociate on a longer time scale, energy exchange reaches equilibrium conditions. These conditions were dubbed (more mellifluously) blackbody infrared radiative dissociation (BIRD) [70], which has since been used to refer to all such experimental measurements and applied to study activation energies for a variety of systems. In one of the earliest BIRD studies, the nonapeptide bradykinin and multiple variants in both singly and doubly charged states were examined, with activation energies ranging from 0.6

UU IR Author Manuscript

– 1.4 eV and Arrhenius A factors covering a seven order of magnitude range [71], as illustrated by the classic Arrhenius plots in Figure 6. A key consideration in such studies is that the approach can be applied to even very large mass species, where the kinetic shifts (delays in the appearance of a product ion associated with the lifetime of the energized molecule, see below) inherent in other determinations could easily lead to inaccurate thermochemistry.

In addition to such equilibrium based infrared (IR) techniques, it is also possible to induce dissociation by absorption of multiple infrared photons in IRMPD, IR multiple photon dissociation, or even single IR photons if the bond in question is weak enough (e.g., in various rare-gas tagging experiments). In general, however, it is difficult to ascertain exactly how many IR photons might be absorbed or to determine a threshold from such absorptions as the spectroscopic details rely on there being a vibrational state that allows absorption. Thus, these experiments generally do not provide thermochemical information, but are a rich source of spectroscopic data.

**Collision-induced Dissociation and Reaction**

"Aston bands" were extraneous mass peaks observed in mass spectrometers and were generally considered to be a nuisance, being broad and ill-resolved. Aston recognized that these extra peaks were the result of collisions inducing a change in the m/z ratio in the field free regions of the mass spectrometer [72]. In the 1960s, the first systematic work on collision-induced dissociation (CID), or collisionally-activated dissociation (CAD), was initiated [73]. In one of the first threshold determinations, reactions (5) with Rg = He, Ne, and Ar were studied as a function of kinetic energy using a "double mass spectrometer" [74].

$$Rg^+ + CO \rightarrow C^+ + O + Rg \qquad \Delta_rH = D(CO) + IE(C) - IE(Rg) \qquad (5)$$

Because of the simplicity of the reactions, the thermochemistry was already known with enthalpies of reaction of -2.21, 0.72, and 6.44 eV, respectively. In accord, reaction of $He^+$ showed a cross section increasing as the energy decreased, whereas $Ne^+$ and $Ar^+$ exhibited energy thresholds where the first observation of product signal agreed with the known

UU IR Author Manuscript

thermochemistry. The authors noted that "since, at present, we have no theory to provide a guide to the proper technique for establishing a threshold energy, it is dangerous to take the onset energy seriously." However, they go on to presciently conclude that "If the method used in the present report proves to have any generality, it appears that it is a technique capable of measuring dissociation energies with an accuracy, perhaps, of 0.1 eV."

An important contribution to collision studies was realized by Chantry, who summarized his finding by stating "the energy resolution achieved in many such experiments is limited by the Doppler width arising from the target gas thermal velocities, rather than by the spread in energy of the primary beam" [75]. Later, Lifshitz et al. laid out formulae combining this Doppler broadening with that associated with the kinetic energy distribution of the ion reactant [76]. The effects of such broadening are nicely illustrated by early studies of reaction (6),

$$C^+ + H_2\,(D_2) \rightarrow CH^+\,(CD^+) + H\,(D) \qquad \Delta_r H = 0.4\ \text{eV} \qquad (6)$$

as shown in Figure 7 [77-81]. It can be seen that the data from Maier, Fennelly, and Koski and coworkers (circles) agrees nicely with cross sections measured in my own laboratory, although earlier measurements of Koski and coworkers (diamonds) differ appreciably. This agreement only occurs when the data are plotted on the original energy scales for all four studies, whereas the three earlier studies had actually reported their data with energy scales shifted by 0.15 – 0.25 eV. This was done so that the linear portion of the rising cross section extrapolated to a threshold of 0.4 eV, the known endothermicity of reaction (6). In contrast, the upper panel of Figure 7 shows that when a reasonable threshold model is chosen and properly convoluted with the Doppler broadening and ion kinetic energy distribution, the data is well reproduced using a threshold that again agrees with the known thermochemistry. More sophisticated treatments of this system including detailed phase space theory treatments and crossed beam experiments followed later [82-84].

Many early studies of endothermic reactions were hampered by the difficulties of producing intense ion beams at low kinetic energies, a result of space charge limitations on focusing slow ions over extended path lengths. Such difficulties were relieved efficiently by the

UU IR Author Manuscript

advent of radio frequency technology, including quadrupoles [85] and "guided ion beams" [86]. (In Figure 7 for instance, note that the older studies include no points below about 0.12 eV, whereas the guided ion beam results extend to about 0.02 eV.) This allowed kinetic energy resolved experiments to become more routine and, when combined in a tandem mass spectrometer configuration, capable of examining a wide range of chemical phenomena [87,88]. For processes (5) and (6), the simplicity of the systems and the nature of the exchange reactions means that these reactions do not exhibit difficulties that become evident in collision-induced dissociation (CID) reactions (7).

$$ML_x^+ + Rg \rightarrow ML_{x-1}^+ + L + Rg \qquad \Delta_r H = D(L_{x-1}M^+–L) \qquad (7)$$

Here, the pressure of the neutral target gas is shown to influence the onsets of endothermic processes. This becomes increasingly obvious as the size of the complex increases. Thus, we first noticed this for dissociation of iron cluster cations, but only clusters containing five or more iron atoms showed the effect [89]. This pressure effect was then quantified in a subsequent study of niobium cluster cations [90], where we first developed the means to eliminate the problem: a simple extrapolation of the data to zero pressure, rigorously single collision conditions. However, this does mean that the reaction cross sections must now be measured at multiple (at least three) pressures, increasing the complexity of the measurements.

Another factor that became more apparent as the complexity of the systems being studied increased was the internal energies of the reactants, which can contribute to the energy available to allow reaction or dissociation to occur. Although this conclusion may seem obvious now, the threshold treatments used in energy resolved mass spectrometry until 1991 focused on the kinetic energy distributions outlined by Chantry and Lifshitz et al., which was adequate for the simple atom-diatom reactions studied dominantly. In my laboratory, the epiphany occurred during our examination of the CID of $Fe^+(CO)_x$ where $x = 1 – 5$ [52]. Here, the sum of these five bond energies was well known (5.90 ± 0.08 eV) because the enthalpies of formation of $Fe^+$, CO, $Fe(CO)_5$, and its ionization energy had been measured accurately. When we first analyzed our CID data, the sum of the five BDEs was much too low (4.74 ± 0.17 eV), and our results

UU IR Author Manuscript

languished for about a year and a half before we began including the internal energy of the reactant ions. Once this distribution was explicitly accounted for, our results (5.82 ± 0.13 eV) matched the literature thermochemistry nicely and we could demonstrate this effect also likely influenced results of photoionization appearance energies of the same system.

The final linchpin in allowing accurate thermodynamics to be obtained from kinetic energy resolved CID is to specifically consider the lifetime for the dissociation kinetics. This issue had long been known with Chupka pointing out the issue for photoionization appearance energy measurements about 50 years ago [46]. In our case, the need to include this feature became obvious as we examined increasingly larger metal cluster cations [89]. This is shown in Figure 8 where it can be seen that the energy for loss of an iron atom continues to grow with cluster size if the lifetime effects are not included, whereas it begins to level out when such effects are accounted for. As such values are anticipated to reach a finite bulk phase value, for iron $\Delta H_{vap}$ = 4.3 eV, the latter behavior is clearly more appropriate. The difference between these threshold energies is the "kinetic shift" associate with the lifetime of the energized cluster and dependent on the instrumentally determined flight time of the ions. Enhancements in the treatment of these effects have also been implemented [91-93].

Additional historical aspects of kinetic energy resolved mass spectrometry as a means to determine thermochemistry include both instrumental developments and advances in the analysis such as identity of the collision partner [94,95], effects of competition [96], and sequential dissociations [97]. Several of these have been recounted in more detail elsewhere [98].

**Dissociation Induced by Electrons**

The possibility of using electrons to induce dissociation was originally explored by Cody and Freiser in a technique they called electron-impact excitation of ions from organics (EIEIO) [99]. This name, chosen primarily because Freiser thought it was funny, has since been deemed obsolete because nomenclature committees have no sense of humor. Despite the potential utility of tuning the electron energy and measuring a thermodynamic onset for dissociation, this process

was never quantified and was used mainly for structural determinations. More recently, the advent of electron capture dissociation (ECD) has become a valuable tool for the study of multiply charged ions [100]. As before, these experiments are geared primarily towards structural elucidation, but some experiments have begun to exploit the possibility of using ECD to measure thermochemistry in hydrated metal complexes [101]. The first such experiments, shown in Figure 9, showed that capture of the electron by hydrated calcium dication induces loss of 10 or 11 water ligands, a fairly narrow range that can be related back to the reduction potential of the metal dication (or recombination energy) coupled with knowledge of the average hydration energy of approximately 0.4 eV per water molecule. Other dissociation processes (BIRD, EIEIO, and CID) occur but yield primarily water loss with no charge reduction. Subsequently, the average binding energy for complexes with more than 40 water molecules has been measured more directly using uv photodissociation as 0.447 ± 0.043 eV (precision of 0.004 eV), independent of the metal dication identity [102]. This is very similar to the bulk enthalpy of vaporization of water, 0.46 eV. This approach has now been refined considerably and there is the promise to provide not only ion thermochemistry, but perhaps definitively establish the absolute standard hydrogen electrode (SHE) potential and determine one-electron reduction potentials for metal dications that fail do so in aqueous solution [103,104].

**Equilibrium Methods**

One of the first mass spectrometers specifically designed to investigate thermodynamic properties by the determination of equilibrium constants as a function of temperature was the high pressure mass spectrometer (HPMS). The earliest such studies found that series of ions separated by 18 mass units were generated, no matter what the gas in the source was [105]! Upon recognizing that this increment must correspond to water, the hydration energies of the proton became the first quantitative thermochemical study using equilibria [106,107]. The advent of pulsed HPMS (PHPMS), in which the ionizing electron beam is pulsed, allowed examination of the kinetics leading to establishment of equilibrium [108]. Soon, studies

UU IR Author Manuscript

included a wide range of systems involving relative measurements of solvation energies, proton affinities, gas-phase acidities, and transfer equilibria of electrons, hydrides, halides, methyl cations, and metal cations.

About the same time HPMS was being developed, parallel accomplishments were achieved using the flowing afterglow technique [109] and ion cyclotron resonance (ICR) mass spectrometry [110]. In both experiments, equilibria can again be established and used to provide thermodynamic data. ICR methods rely on trapping [111] techniques, which allow the convenient establishment of equilbria [112], and double resonance methods [113], which allow determination of which direction is exothermic. In the case of ICR, the first measurements of metal cation affinities, specifically $Li^+$ [114], were made.

As long as a true equilibrium is established (and remains unperturbed by probing the ion concentrations), such methods can provide among the most accurate thermodynamic information, albeit restricted to *relative* values. Also the range of such experiment is fairly narrow, as imposed by the accessible temperature range. However, by overlapping experiments, extensive "ladders" of thermochemical data can be assembled [115], although cumulative uncertainties can affect values at the ends of such ladders. In the end, such databases require absolute values (ideally several arrayed throughout the ladder) determined using other techniques (primarily those described above) in order to anchor them (see for example, [6]).

In some systems, the differences in the affinities of interest are too large to allow for a true equilibrium to be achieved. Here, bracketing methods can be used to roughly determine the thermodynamic value of interest. For example, the ion ($M^{+/-}$) affinity of an unknown (A) can be bracketed by species with known ion affinities above ($B_1$) and below ($B_2$) that of A.

$$M^{+/-}(B_1) + A \rightarrow M^{+/-}(A) + B_1 \qquad \Delta_r H > 0 \qquad (8)$$

$$M^{+/-}(B_2) + A \rightarrow M^{+/-}(A) + B_2 \qquad \Delta_r H < 0 \qquad (9)$$

To be rigorous, such reactions should be examined in both the forward and reverse directions to avoid problems associated with side reactions, alternative products, or barriers. Although the concept was originally developed by Tal'roze and Frankevich some 50 years ago [116],

quantitative use of the bracketing method required development of more extensive thermodynamic tables. In one early application, ICR was used to measure proton transfer rates between $CHF_2^+$ and seven compounds with known proton affinities to ascertain PA($CF_2$) as 720 ± 8 kJ/mol [117]. One means of potentially improving on the simple bracketing method is to parameterize the expected reaction efficiency with the free energy of reaction, as explored by Bouchoux and coworkers [118]. This allows data from several reactions to be simultaneously considered, permitting a more exact identification of the likely thermochemical quantity. As for Cook's kinetic method, Bouchoux's thermokinetic approach relies on several assumptions as well as an effective temperature and hence the same general provisos on the results hold.

**Association**

Bond dissociation energies can also be determined from the reverse of the dissociation reaction, i.e., association of two species, because the lifetime of the association complex depends critically on the bond energy between these species [119,120]. This method requires detailed modeling of the kinetics and is generally examined in the limit of no collisional stabilization by extrapolation of finite pressure data. Dunbar and coworkers have used this method to measure the binding energies of $NO^+$ and metal ions to aromatic molecules, e.g., $Cr^+$ to $C_6H_{6-x}F_x$ for $x$ = 0 – 6 [121]. Their value for D($Cr^+$–benzene) of 1.93 eV is in reasonable agreement with that obtained from TCID experiments, 1.76 ± 0.10 eV [122], and shows that fluorination decreases the bond energy by about 0.18 eV per fluorine, consistent with the electron withdrawing character of the halogen.

One difficulty with such measurements is that they rely on a single rate constant measurement, the radiative association rate at the ambient temperature. A more sensitive test is provided by examining the kinetic energy dependence of the association process [123]. Figure 10 shows the example of association of dimethoxyethane (DXE, $CH_3OCH_2CH_2OCH_3$) with $Cu^+$ analyzed using phase space theory (PST) where all three reactive channels are modeled simultaneously [124]. It can be seen that the cross sections for all three reactive channels are

reproduced well over extended energy and magnitude ranges. The thermochemistry obtained from this modeling yields the bond energies, $D(Cu^+\text{-DXE}) = 2.85 \pm 0.23$ eV, $D(CuH{-}C_4H_9O_2^+) = 2.69 \pm 0.19$ eV, and $D(CuC_3H_6O^+{-}CH_3OH) = 2.28 \pm 0.17$ eV, which agrees well with data taken from a TCID study of the $Cu^+(DXE)$ complex, $2.79 \pm 0.07$, $2.70 \pm 0.08$, and $2.0 \pm 0.6$ eV, respectively [125].

**Neutrals**

Quite naturally, mass spectrometric methods generally focus on determining the thermodynamic properties of ionic species. However, such methods are often easily extended to measure the thermochemistry of neutrals. A review article that provides an excellent example of several approaches is "Three Methods To Measure RH Bond Energies" [126]. The first method is acidity cycles, which refer to measurements of the acidity of the RH molecule, reaction (10).

$$RH \rightarrow R^- + H^+ \qquad \Delta_r H = \Delta_{acid}H(RH) \qquad (10)$$

As discussed above, this can be achieved routinely by equilibrium methods in which protons are exchanged between anions. The RH bond energy is obtained by combining the measured acidity with IE(H) and EA(R), equation (11).

$$D(R{-}H) = \Delta_{acid}H(RH) - IE(H) + EA(R) \qquad (11)$$

The second method is photoionization mass spectrometry in which the appearance energy of $R^+$ from RH, $AE(R^+,RH)$, is measured using the methods outlined above. The RH bond energy is obtained by combining this value with IE(R), equation (12).

$$D(R{-}H) = AE(R^+,RH) - IE(R) \qquad (12)$$

The third method is radical kinetics, in which the enthalpy of reaction (13), where X is usually a halogen atom, is determined.

$$RH + X \rightarrow R + HX \qquad \Delta_r H = D(X{-}H) - D(R{-}H) \qquad (13)$$

The RH bond energy is obtained by combining this value with the known HX bond energy to give D(R–H). Clearly, this method need not require mass spectrometry, and indeed, in the earliest experiments, fluorescence spectroscopy was commonly used to monitor the decay in the

UU IR Author Manuscript

population of X [127]. As a consequence, only the forward reaction rate was actually measured, such that assumptions about the thermodynamics of the reverse reaction were needed (generally assumed to equal zero). Improvements in the thermochemistry evolving from the radical kinetics method relied on measuring both forward and reverse reaction rates using mass spectrometric methods (to measure the amounts of X and R, for example) [128]. These measurements demonstrated that the early assumptions made for the reverse activation energy were inaccurate and resolved long standing discrepancies among the three methods [128]. Ultimately, then, all three methods now rely on mass spectrometry to acquire the neutral thermochemistry.

Another interesting means of determining neutral thermochemistry is photofragment translational spectroscopy (PTS), mentioned above. Internal states of the species can be identified from features in the wavelength dependence of the photodissociation and the maximum kinetic energy of the fragments (which are detected by ionization and mass spectrometry) allows determination of the bond energies of stable neutrals [129]. Radicals can also be probed, for example, photodetachment of $CH_3S^-$ leads to the $CH_3S$ radical, which is photodissociated and exhibits extensive vibrational structure [130]. The maximum kinetic energy of the photofragments leads to assignment of $D_0(CH_3–S) = 3.045 \pm 0.015$ eV. Combined with the enthalpies of formation of H, S, $CH_3$, and $CH_3SH$, the enthalpy of formation of $CH_3S$ ($1.346 \pm 0.018$ eV) and $D_{298}(CH_3S–H) = 3.775 \pm 0.017$ eV are obtained [8], in good agreement with values from radical kinetics measurements of $1.363 \pm 0.023$ eV and $3.788 \pm 0.016$ eV, respectively [131].

These methods generally focus on the thermochemistry of stable molecules or the radicals produced from them. Additional open shell species can also be examined, for example, by measuring the thermodynamics for ligand transfer. For example, reactions (14) have been used to determine bond energies for neutral metal hydrides (L = H and RL = alkanes and acids) [132-139], metal methyls (L = $CH_3$ and RL = alkanes) [135,137], and metal oxides (L = O and RL = $NO_2$ and c-$C_2H_4O$) [30,136,140,141] either by bracketing [132-134] or threshold determinations [30,135-141].

$$M^+ + RL \rightarrow ML + R^+ \qquad \Delta_r H = D(RL) - D(ML) + IE(R) - IE(M) \qquad (14a)$$

$$M^- + RL \rightarrow ML + R^- \qquad \Delta_r H = D(RL) - D(ML) + EA(M) - EA(R) \qquad (14b)$$

For the metal hydrides, comparisons of results from these methods with those from spectroscopic studies and high temperature (Knudsen cell) mass spectrometry (HTMS) verify the accuracy of this mass spectrometric approach [142]. HTMS has also been used to study a variety of equilibria at high temperatures, accessing information for refractory species that are often unavailable using other methods [143]. Often the accuracy of this thermochemistry is limited by the large extrapolation needed to go from the experimental temperature range of 1000 – 2500 K back to 300 K.

Of course, it is also possible to combine measurements of ionization energies (or electron affinities) with values of cationic (anionic) bond dissociation energies to obtain BDEs for neutral species, as in equation (15) for cations.

$$D(R–L) = D(R^+–L) + IE(RL) - IE(R) \qquad (15)$$

In some cases, these approaches rival or outperform direct measurements of the neutral BDES. For example, the best values for D(CuO) come from determination of the threshold for reaction (16), which yields 2.94 ± 0.12 eV [141], or by combining $D(CuO^+)$ = 1.35 ± 0.12 eV from the endothermic reaction (17) [141] with IE(CuO) = 9.41 ± 0.01 eV [26] and IE(Cu) = 7.72634 eV to yield the consistent D(CuO) = 3.03 ± 0.12 eV value. The one high temperature mass spectrometry study had provided a value of 2.76 ± 0.22 eV [144], which again is consistent but less precise.

$$Cu^+ + NO_2 \rightarrow CuO + NO^+ \qquad (16)$$

$$\rightarrow CuO^+ + NO \qquad (17)$$

In other cases, combining cationic bond energies with ionization energies provides the only means presently available for determining some neutral thermochemistry, e.g., such values comprise most of the known thermochemistry for neutral transition metal clusters [145].

**Conclusion**

The last half century has seen extensive advances in the use of mass spectrometry to ascertain thermodynamic information about anions, cations, and neutrals of all types. Increases in the accuracy and precision of this information has been realized via both instrumental developments and the tools used to analyze the data. In many cases, the most accurate and precise techniques are restricted to small systems, but increasingly large systems are being tackled with success. This trend will undoubtedly continue for the next half century, with ever larger systems being examined and quality thermodynamic information extracted. The challenge remains to maintain the accuracy and precision of this thermochemistry as the limits of the instrumentation and theory used to understand the resultant information are stretched. In the rush to acquire such quantitative data, which is so useful in making predictions and understanding the systems of interest, researchers need to be mindful that inaccurate thermodynamic information is actually problematic and more useless than the absence of that information.

**Acknowledgement**. Our work in the area of ion thermochemistry has long been funded by the National Science Foundation, Grant No. CHE-1049580, and the Chemical Sciences, Geosciences, and Biosciences Division, Office of Basic Energy Sciences, U. S. Department of Energy. The author gratefully acknowledges his many coworkers contributing to this endeavor.

UU IR Author Manuscript

**References**

[1] J.J. Thomson, Proceed. Roy. Soc. A 89 (1913) 1.

[2] E. Goldstein, Berlin Akd. Monatsber II (1886) 691.

[3] W. Wien, Ann. der Physik 8 (1902) 244.

[4] F.H. Field, J.L. Franklin, Electron Impact Phenomena and the Properties of Gaseous Ions, Academic Press, New York, 1957.

[5] S.G. Lias, J.E. Bartmess, J.F. Liebman, J.L. Holmes, R.D. Levin, W.G. Mallard, J. Phys. Chem. Ref. Data Suppl. 1 17 (1988) 1.

[6] E.P.L. Hunter, S.G. Lias, J. Phys. Chem. Ref. Data 27 (1998) 413.

[7] P.J. Linstrom, W.G. Mallard, "NIST Chemistry WebBook, NIST Standard Reference Database Number 69", National Institute of Standards and Technology, Gaithersburg MD, 20899, http://webbook.nist.gov, (retrieved March 6, 2014).

[8] K.M. Ervin, Chem. Rev. 101 (2001) 391.

[9] A.C.G. Mitchell, Z. Physik 50 (1928) 570.

[10] J.E. Bartmess, J. Phys. Chem. 98 (1994) 6420.

[11] E.P. Wigner, Phys. Rev. 73 (1948) 1002.

[12] K. Watanabe, J. Chem. Phys. 22 (1954) 1564.

[13] H.M. Rosenstock, K. Draxl, B.W. Steiner, J.T. Herron, J. Phys. Chem. Ref. Data 6 (Suppl. 1) (1977) 1.

[14] H. Hurzeler, M.G. Inghram, J.D. Morrison, J. Chem. Phys. 28 (1958) 76.

[15] B.L. Kurbatov, F.I. Vilesov, A.N. Terenin, Soviet Phys.-Doklady 6 (1961) 490.

[16] D.W. Turner, M.I. Al Jobory, J. Chem. Phys. 37 (1962) 3007.

[17] D. Villarejo, R.R. Herm, M.G. Inghram, J. Chem. Phys. 46 (1967) 4995.

[18] B.P. Brehm, E. V., Z. Naturforsch., Teil A 22 (1967) 8.

[19] C.Y. Ng, Int. J. Mass Spectrom. 200 (2000) 357.

UU IR Author Manuscript

[20] T.B.B. W. B. Peatman, E. W. Schlag, E. W., Chem. Phys. Lett. 3 (1969) 492.

[21] T.P. Baer, W. B., E.W. Schlag, Chem. Phys. Lett. 4 (1969) 243.

[22] K. Müller-Dethlefs, M. Sander, E.W. Schlag, Chem. Phys. Lett. 112 (1984) 291.

[23] H.J. Neusser, H. Drause, Int. J. Mass Spectrom. 131 (1994) 211.

[24] S.R. Long, J.T. Meek, J.P. Reilly, J. Chem. Phys. 79 (1983) 3206.

[25] G.K. Jarvis, K.-M. Weitzel, M. Malow, T. Baer, Y. Song, C.Y. Ng, Review of Scientific Instruments 70 (1999) 3892.

[26] R.B. Metz, C. Nicolas, M. Ahmed, S.R. Leone, J. Chem. Phys. 123 (2005) 114313.

[27] E.R. Fisher, P.B. Armentrout, J. Phys. Chem. 94 (1990) 4396.

[28] D.E. Clemmer, P.B. Armentrout, J. Chem. Phys. 97 (1992) 2451.

[29] K.S. Haber, J.W. Zwanziger, F.X. Campos, R.T. Wiedmann, E.R. Grant, Chem. Phys. Lett. 144 (1988) 58.

[30] D.E. Clemmer, N.F. Dalleska, P.B. Armentrout, J. Chem. Phys. 95 (1991) 7263.

[31] L.M. Branscomb, S.J. Smith, Phys. Rev. 98 (1955) 1127.

[32] W.C. Lineberger, B.W. Woodward, Physical Review Letters 25 (1970) 424.

[33] L.M. Branscomb, D.S. Burch, S.J. Smith, S. Geltman, Phys. Rev. 111 (1958) 504.

[34] D.M. Neumark, K.R. Lykke, T. Andersen, W.C. Lineberger, Phys. Rev. A 32 (1985) 1890.

[35] J.D.D. Martin, J.W. Hepburn, Physical Review Letters 79 (1997) 3154.

[36] M.W. Chase, C.A. Davies, J.R. Downey, D.J. Frurip, R.A. McDonald, A.N. Syverud, J. Phys. Chem. Ref. Data 14 (1985) Suppl. 1.

[37] J.D.D. Martin, J.W. Hepburn, J. Chem. Phys. 109 (1998) 8139.

[38] B. Brehm, M.A. Gusinow, J.L. Hall, Phys. Rev. Lett. 19 (1967) 737.

[39] M.W. Siegel, R.J. Celotta, J.L. Hall, J. Levine, R.A. Bennett, Phys. Rev. A 6 (1972) 607.

[40] T.N. Kitsopoulos, I.M. Waller, J.G. Loeser, D.M. Neumark, Chem. Phys. Lett. 159 (1989) 300.

[41] G. Drechsler, U. Boesl, C. Bassmann, E.W. Schlag, J. Chem. Phys. 107 (1997) 2284.

[42] A. Osterwalder, M.J. Nee, J. Zhou, D.M. Neumark, J. Chem. Phys. 121 (2004) 6317.

[43] I. León, Z. Yang, L.S. Wang, J. Chem. Phys. 138 (2013) 184304.

[44] G.F. Gantefor, D.M. Cox, A. Kaldor, J. Chem. Phys. 93 (1990) 8395.

[45] J. Ho, K.M. Ervin, W.C. Lineberger, J. Chem. Phys. 93 (1990) 6987.

[46] W.A. Chupka, J. Chem. Phys. 30 (1959) 191.

[47] C. Lifshitz, F.A. Long, J. Chem. Phys. 41 (1964) 2468.

[48] B. Sztaray, T. Baer, J. Phys. Chem. A 106 (2002) 8046.

[49] S. Goebel, C.L. Haynes, F.A. Khan, P.B. Armentrout, J. Am. Chem. Soc. 117 (1995) 6994.

[50] P.A.M. van Koppen, M.T. Bowers, J.L. Beauchamp, D.V. Dearden, ACS Symp. Series 428 (1990) 34.

[51] C.J. Carpenter, P.A.M. van Koppen, M.T. Bowers, J. Am. Chem. Soc. 117 (1995) 10976.

[52] R.H. Schultz, K.C. Crellin, P.B. Armentrout, J. Am. Chem. Soc. 113 (1991) 8590.

[53] F.A. Khan, D.L. Steele, P.B. Armentrout, J. Phys. Chem. 99 (1995) 7819.

[54] R.G. Cooks, T.L. Kruger, J. Am. Chem. Soc. 99 (1977) 1279.

[55] X. Cheng, Z. Wu, C. Fenselau, J. Am. Chem. Soc. 115 (1993) 4844.

[56] P.B. Armentrout, J. Am. Soc. Mass Spectrom. 11 (2000) 371.

[57] P.B. Armentrout, J. Mass Spectrom. 34 (1999) 74.

[58] L. Drahos, K. Vekey, J. Mass Spectrom. 34 (1999) 79.

[59] R.G. Cooks, J.T. Koskinen, P.D. Thomas, J. Mass Spectrom. 34 (1999) 85.

[60] Y.A. Ranasinghe, I.B. Surjasasmita, B.S. Freiser, in Organometallic Ion Chemistry Eds., B.S. Freiser, Kluwer, Dordrecht, 1996, pp. 229.

[61] A.M. Wodtke, Y.T. Lee, J. Phys. Chem. 89 (1985) 4744.

[62] D.L. Osborn, D.J. Leahy, D.R. Cyr, D.M. Neumark, J. Chem. Phys. 104 (1996) 5026.


UU IR Author Manuscript

[63] K. Hiraoka, J. Chem. Phys. 89 (1988) 3190.

[64] K.A.H. C. R. Sherwood, M. C. Garner, K. M. Strong, and R. E. Continetti, J. Chem. Phys. 105 (1996) 10803.

[65] R.C. Dunbar, J. Phys. Chem. 91 (1987) 2801.

[66] R.C. Dunbar, C. Lifshitz, J. Chem. Phys. 94 (1991) 3542.

[67] R.C. Dunbar, J. Phys. Chem. 98 (1994) 8705.

[68] R.C. Dunbar, T.B. McMahon, D. Thoelmann, D.S. Tonner, D.R. Salahub, D. Wei, J. Am. Chem. Soc. 117 (1995) 12819.

[69] R.C. Dunbar, T.B. McMahon, Science 279 (1998) 194.

[70] W.D. Price, P.D. Schnier, E.R. Williams, Anal. Chem. 68 (1996) 859.

[71] P.D. Schnier, W.D. Price, R.A. Jockusch, E.R. Williams, J. Am. Chem. Soc. 118 (1996) 7178.

[72] F.W. Aston, Mass Spectra and Isotopes, Edward Arnold, London, 1942.

[73] K.R. Jennings, Int. J. Mass Spectrom. 200 (2000) 479.

[74] C.F. Giese, W.B. Maier, J. Chem. Phys. 39 (1963) 197.

[75] P.J. Chantry, J. Chem. Phys. 55 (1971) 2746.

[76] C. Lifshitz, R.L.C. Wu, T.O. Tiernan, D.T. Terwilliger, J. Chem. Phys. 68 (1978) 247.

[77] W.B. Maier, J. Chem. Phys. 46 (1967) 4991.

[78] P.F. Fennelly, Ph.D. thesis, Brandeis University, Ann Arbor, MI, 1972.

[79] E. Lindemann, L.C. Frees, R.W. Rozett, W.S. Koski, J. Chem. Phys. 56 (1972) 1003.

[80] L.C. Frees, P.L. Pearl, W.S. Koski, Chem. Phys. Lett. 63 (1979) 108.

[81] K.M. Ervin, P.B. Armentrout, J. Chem. Phys. 80 (1984) 2978.

[82] K.M. Ervin, P.B. Armentrout, J. Chem. Phys. 84 (1986) 6738.

[83] K.M. Ervin, P.B. Armentrout, J. Chem. Phys. 84 (1986) 6750.

[84] D. Gerlich, R. Disch, S. Scherbarth, J. Chem. Phys. 87 (1987) 350.


UU IR Author Manuscript

[85] U. von Zahn, H. Tatarczyk, Phys. Lett. 12 (1964) 190.

[86] E. Teloy, D. Gerlich, Chem. Phys. 4 (1974) 417.

[87] K. Ervin, S.K. Loh, N. Aristov, P.B. Armentrout, J. Phys. Chem. 87 (1983) 3593.

[88] K.M. Ervin, P.B. Armentrout, J. Chem. Phys. 83 (1985) 166.

[89] S.K. Loh, D.A. Hales, L. Lian, P.B. Armentrout, J. Chem. Phys. 90 (1989) 5466.

[90] D.A. Hales, L. Lian, P.B. Armentrout, Int. J. Mass Spectrom. Ion Processes 102 (1990) 269.

[91] F.A. Khan, D.E. Clemmer, R.H. Schultz, P.B. Armentrout, J. Phys. Chem. 97 (1993) 7978.

[92] M.T. Rodgers, K.M. Ervin, P.B. Armentrout, J. Chem. Phys. 106 (1997) 4499.

[93] P.B. Armentrout, K.M. Ervin, M.T. Rodgers, J. Phys. Chem. A 112 (2008) 10071.

[94] N. Aristov, P.B. Armentrout, J. Phys. Chem. 90 (1986) 5135.

[95] D.A. Hales, P.B. Armentrout, J. Cluster Science 1 (1990) 127.

[96] M.T. Rodgers, P.B. Armentrout, J. Chem. Phys. 109 (1998) 1787.

[97] P.B. Armentrout, J. Chem. Phys. 126 (2007) 234302.

[98] P.B. Armentrout, Int. J. Mass Spectrom. Ion Processes 200 (2000) 219.

[99] R.B. Cody, B.S. Freiser, Anal. Chem. 51 (1979) 547.

[100] R.A. Zubarev, N.L. Kelleher, F.W. McLafferty, J. Am. Chem. Soc. 120 (1998) 3265.

[101] R.D. Leib, W.A. Donald, M.F. Bush, J.T. O'Brien, E.R. Williams, J. Am. Chem. Soc. 129 (2007) 4894.

[102] W.A. Donald, R.D. Leib, M. Demireva, B. Negru, D.M. Neumark, E.R. Williams, J. Phys. Chem. A 115 (2011) 2.

[103] W.A. Donald, R.D. Leib, M. Demireva, J.T. O'Brien, J.S. Prell, E.R. Williams, J. Am. Chem. Soc. 131 (2009) 13328.

[104] W.A. Donald, E.R. Williams, in Electroanalytical Chemistry: A Series of Advances, Eds., A.J. Bard, C.G. Zosk, CRC Press, Boca Raton, 2014, pp. 1.

[105] P. Kebarle, Int. J. Mass Spectrom. 200 (2000) 313.


UU IR Author Manuscript

[106] P. Kebarle, A.M. Hogg, J. Chem. Phys. 42 (1965) 798.

[107] P.S. Kebarle, S. K., A. Zolla, J. Scarborough, M. Arshadi, J. Am. Chem. Soc. 89 (1967) 6393.

[108] D.A. Durden, P. Kerbarle, A. Good, J. Chem. Phys. 50 (1969) 805.

[109] E.E. Ferguson, F.C. Fehsenfeld, A.L. Schmmeltekopf, Adv. At. Mol. Phys. 5 (1969) 1.

[110] J.L. Beauchamp, Annual Review of Physical Chemistry 22 (1971) 527.

[111] R.T. McIver, Rev. Sci. Instrum. 41 (1970) 555.

[112] D.H. Aue, M.T. Bowers, H.M. Webb, R.T. McIver, J. Am. Chem. Soc. 93 (1971) 4314.

[113] L.R. Anders, J.L. Beauchamp, R.C. Dunbar, J.D. Baldeschwieler, J. Chem. Phys. 45 (1966) 1062.

[114] R.D. Wieting, R.H. Staley, J.L. Beauchamp, J. Am. Chem. Soc. 97 (1975) 924.

[115] T.B. McMahon, Int. J. Mass Spectrom. 200 (2000) 187.

[116] V.L. Tal'roze, E.L. Frankevich, Dokl. Acad. Nauk. 111 (1956) 376.

[117] J. Vogt, J.L. Beauchamp, J. Am. Chem. Soc. 97 (1975) 6682.

[118] G. Bouchoux, J.Y. Salpin, D. Leblanc, Int. J. Mass Spectrom. Ion Processes 153 (1996) 37.

[119] R.C. Dunbar, Int. J. Mass Spectrom. Ion Process. 100 (1990) 423.

[120] S.J. Klippenstein, Y.-C. Yang, V. Ryzhov, R.C. Dunbar, J. Chem. Phys. 104 (1996) 4502.

[121] V. Ryzhov, C.-N. Yang, S.J. Klippenstein, R.C. Dunbar, Int. J. Mass Spectrom. 185-187 (1999) 913.

[122] F. Meyer, F.A. Khan, P.B. Armentrout, J. Am. Chem. Soc. 117 (1995) 9740.

[123] H. Koizumi, P.B. Armentrout, J. Chem. Phys. 119 (2003) 12819.

[124] H. Koizumi, F. Muntean, P.B. Armentrout, J. Chem. Phys. 120 (2004) 756.

[125] H. Koizumi, P.B. Armentrout, J. Am. Soc. Mass Spectrom. 12 (2001) 480.

[126] J. Berkowitz, G.B. Ellison, D. Gutman, J. Phys. Chem. 98 (1994) 2744.

[127] D.F. McMillen, D.M. Golden, Annu. Rev. Phys. Chem. 33 (1982) 493.

[128] J.J. Russell, J.A. Seetula, D. Gutman, J. Am. Chem. Soc. 110 (1988) 3092.

[129] D.H. Mordaunt, M.N. Ashfold, J. Chem. Phys. 101 (1994) 2630.

[130] R.T. Bise, H. Choi, H.B. Pedersen, D.H. Mordaunt, D.M. Neumark, J. Chem. Phys. 110 (1999) 805.

[131] J.M. Nicovich, K.D. Dreutter, C.A. van Dijk, P.H. Wine, J. Phys. Chem. 96 (1992) 2518.

[132] L. Sallans, K. Lane, R.R. Squires, B.S. Freiser, J. Am. Chem. Soc. 105 (1983) 6352.

[133] L. Sallans, K.R. Lane, R.R. Squires, B.S. Freiser, J. Am. Chem. Soc. 107 (1985) 4379.

[134] M.A. Tolbert, J.L. Beauchamp, J. Phys. Chem. 90 (1986) 5015.

[135] R. Georgiadis, E.R. Fisher, P.B. Armentrout, J. Am. Chem. Soc. 111 (1989) 4251.

[136] E.R. Fisher, P.B. Armentrout, J. Phys. Chem. 94 (1990) 1674.

[137] E.R. Fisher, P.B. Armentrout, J. Am. Chem. Soc. 114 (1992) 2039.

[138] Y.M. Chen, D.E. Clemmer, P.B. Armentrout, J. Chem. Phys. 95 (1991) 1228.

[139] Y.M. Chen, D.E. Clemmer, P.B. Armentrout, J. Chem. Phys. 98 (1993) 4929.

[140] D.E. Clemmer, M.E. Weber, P.B. Armentrout, J. Phys. Chem. 96 (1992) 10888.

[141] M.T. Rodgers, B. Walker, P.B. Armentrout, Int. J. Mass Spectrom. 182-183 (1999) 99.

[142] P.B. Armentrout, L.S. Sunderlin, in Transition Metal Hydrides, Eds., A. Dedieu, VCH, New York, 1992, pp. 1.

[143] J. Drowart, C. Chatillon, J. Hastie, D. Bonnell, Pure Appl. Chem. 77 (2005) 683.

[144] J.B. Pedley, E.M. Marshall, J. Phys. Chem. Ref. Data 12 (1983) 967.

[145] P.B. Armentrout, Ann. Rev. Phys. Chem. 52 (2001) 423.

[146] L. Lian, C.X. Su, P.B. Armentrout, J. Chem. Phys. 97 (1992) 4072.


UU IR Author Manuscript

**Figure Captions**

**Figure 1.** Spectra for ionization of benzene using time-of-flight photoelectron spectroscopy (top), photoionization efficiency (middle), and zero electron kinetic energy photoelectron spectroscopy (bottom). Labels mark the origin 0-0 transition and two vibrational states of the ion. (Reprinted with permission from H.J. Neusser, H. Drause, Int. J. Mass Spectrom. 131 (1994) 211. Copyright (1994), Elsevier.)

**Figure 2.** Photodetachment cross sections of atomic oxygen negative ions versus photon energy (part a) and frequency (part b) (upper axis shows photon energy in eV). (Reprinted with permission from L.M. Branscomb, D.S. Burch, S.J. Smith, S. Geltman, Phys. Rev. 111 (1958) 504. Copyright (1958), American Institute of Physics. Reprinted with permission from D.M. Neumark, K.R. Lykke, T. Andersen, W.C. Lineberger, Phys. Rev. A 32 (1985) 1890. Copyright (1985), American Institute of Physics.)

**Figure 3.** Breakdown curves of the three consecutive carbonyl-loss and one parallel NO loss steps from photoionized $Co(CO)_3NO$. Experimental data are shown by the dots (including uncertainties) and lines show the results of kinetic modeling. Arrows indicate the derived threshold energies. (Reprinted with permission from B. Sztaray, T. Baer, J. Phys. Chem. A 106 (2002) 8046. Copyright (2002), American Chemical Society.)

**Figure 4.** Photofragment translational spectrum for $N_2O_2^-$ at 570 nm. Data are shown by triangles, with an empirical fit given by the full line, and a prior distribution indicated by the dashed line. The $\nu_2$ (bend) vibrational energy levels for $N_2O$ are shown at the top. (Reprinted with permission from D.L. Osborn, D.J. Leahy, D.R. Cyr, D.M. Neumark, J. Chem. Phys. 104 (1996) 5026. Copyright (1996), AIP Publishing LLC.)

UU IR Author Manuscript

**Figure 5.** Dissociation rate constants from TRPD (375 K) and PEPICO (300 K) for the *p*-iodotoluene ion. Lines are predicted RRKM rate-energy curves assuming a dissociation energy of 1.9 eV corrected for the thermal internal energy at the temperatures noted, and for IR radiative relaxation (Rad). (Reprinted with permission from R.C. Dunbar, C. Lifshitz, J. Chem. Phys. 94 (1991) 3542. Copyright (1991), AIP Publishing LLC.)

**Figure 6.** Arrhenius plot for the dissociation of singly protonated bradykinin (solid circles), des-$Arg^1$-bradykinin (open squares), des-$Arg^9$-bradykinin (solid squares), methyl ester of des-$Arg^9$-bradykinin (solid triangles), Lys-bradykinin (open triangles), and doubly protonated bradykinin (open circles). (Reprinted with permission from P.D. Schnier, W.D. Price, R.A. Jockusch, E.R. Williams, J. Am. Chem. Soc. 118 (1996) 7178. Copyright (1996), American Chemical Society.)

**Figure 7.** Cross section for the reaction $C^+ + H_2 (D_2) \rightarrow CH^+ (CD^+) + H (D)$ as a function of kinetic energy in the laboratory (upper scale) and center-of-mass (lower scale) frames. The upper panel shows the guided ion beam data for the $H_2$ reaction from [81] with the threshold model for reactants having well-defined kinetic energies (broken line) and for the model including the kinetic energy distribution of the reactants (solid line). The lower panel compares that data (solid line) with literature results for $H_2$ (solid symbols) and $D_2$ (open symbols) from Maier [77], Fennelly [78] and Koski and coworkers ([80] circles and [79] diamonds). (Reprinted with permission from K.M. Ervin, P.B. Armentrout, J. Chem. Phys. 80 (1984) 2978. Copyright (1984), AIP Publishing LLC.)

**Figure 8.** Collision-induced dissociation threshold energies measured for loss of an iron atom from $Fe_n^+$ clusters determined with (solid circles) and without (open circles) consideration of lifetime effects. Data taken from [146].

UU IR Author Manuscript

**Figure 9.** Spectra of $Ca^{2+}(H_2O)_{32}$ measured without (top, showing extent of BIRD, collision and electron induced dissociation) and with (bottom, showing loss of 10 and 11 water molecules) electrons injected into the ICR cell. (Reprinted with permission from R.D. Leib, W.A. Donald, M.F. Bush, J.T. O'Brien, E.R. Williams, J. Am. Chem. Soc. 129 (2007) 4894. Copyright (2007), American Chemical Society.)

**Figure 10.** Comparisons of the experimental data with models for the association reaction of $Cu^+$ with DXE as a function of kinetic energy in the center-of-mass frame (lower *x* axis) and laboratory frame (upper *x* axis). Symbols show zero pressure extrapolated cross sections for the indicated processes. Solid lines show the phase space theory (PST) model to all three channels. The dashed line indicates the model cross section for the dark channel back to reactants. The collision (LGS) cross section is also indicated. (Reprinted with permission from H. Koizumi, F. Muntean, P.B. Armentrout, J. Chem. Phys. 120 (2004) 756. Copyright (2004), American Institute of Physics.)

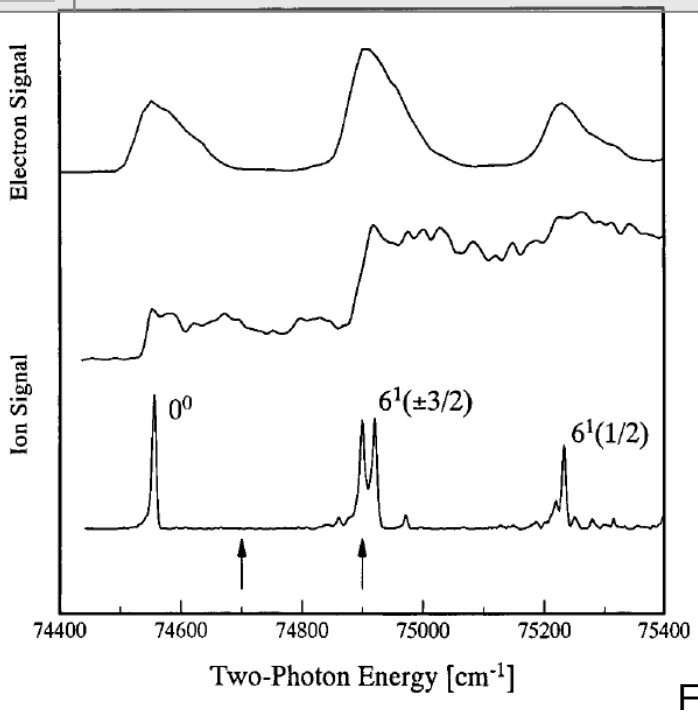


Figure 1

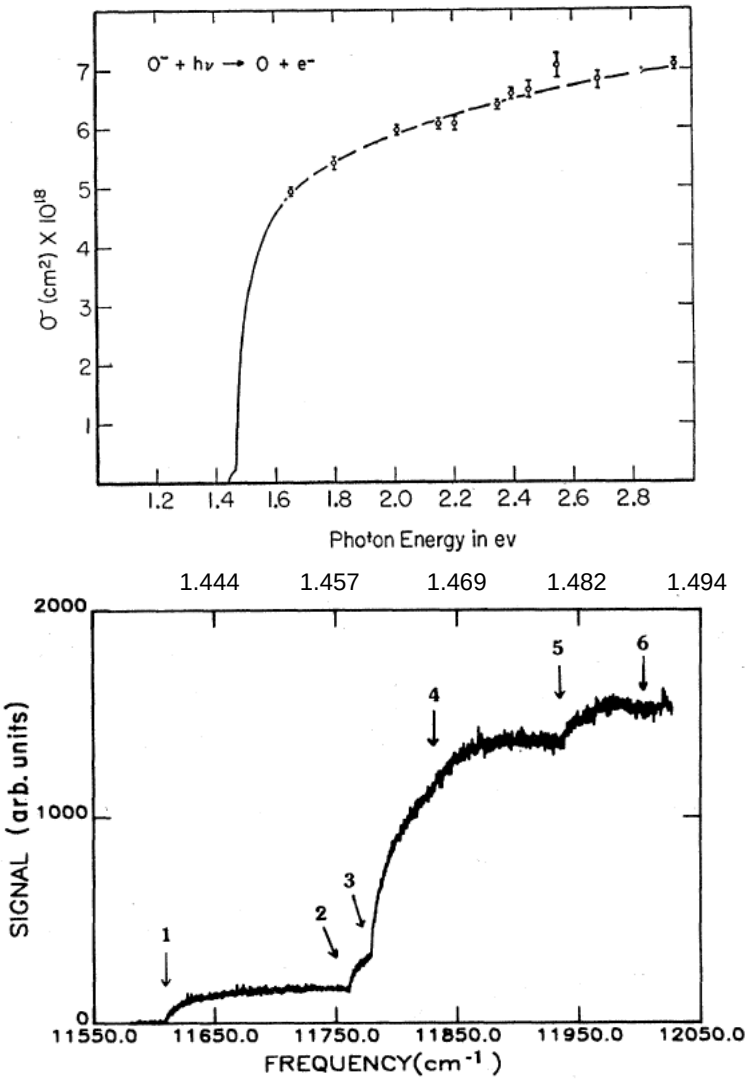


Figure 2

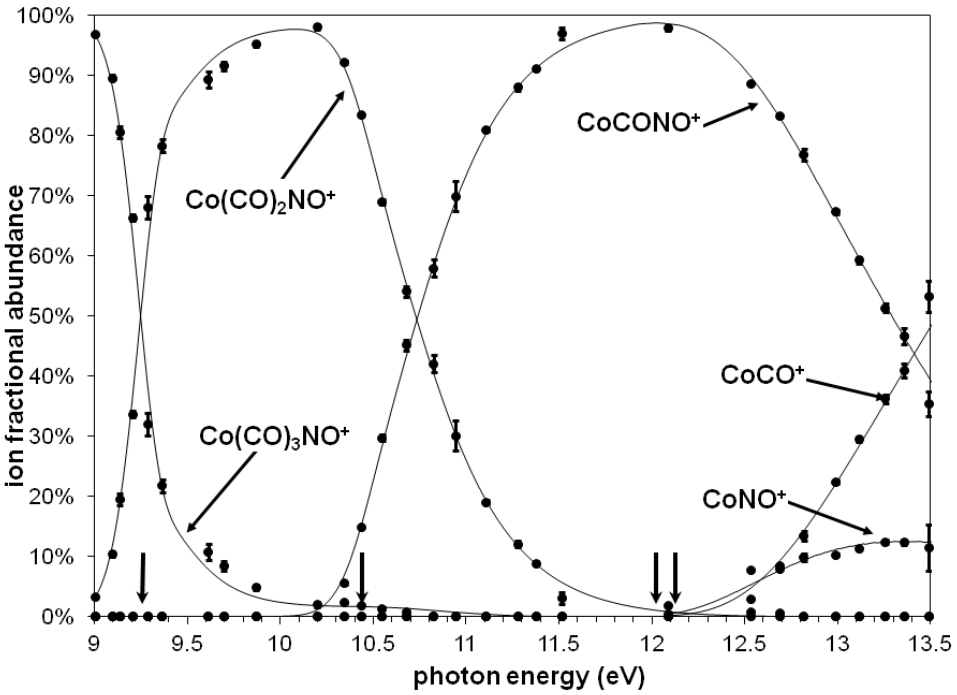


Figure 3

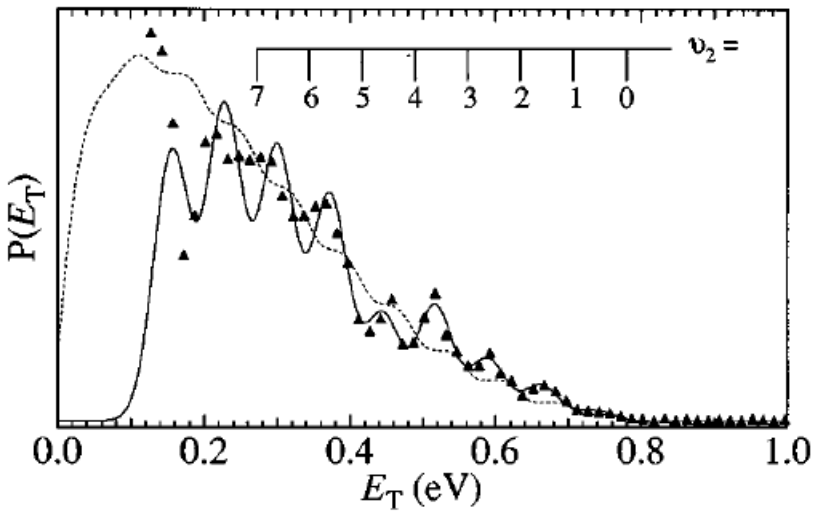


Figure 4

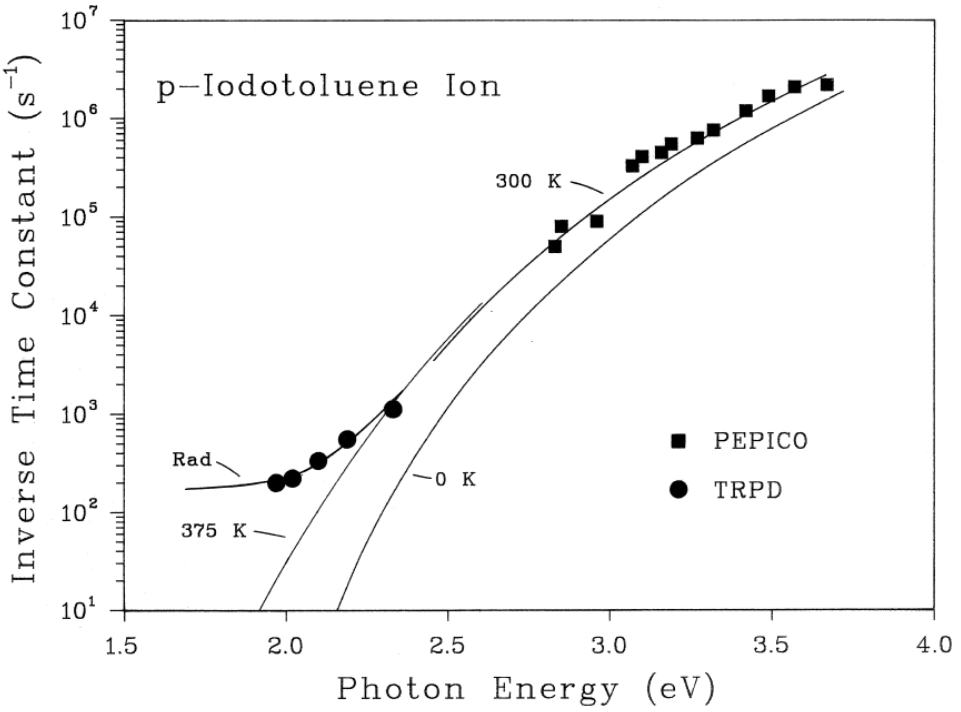


Figure 5

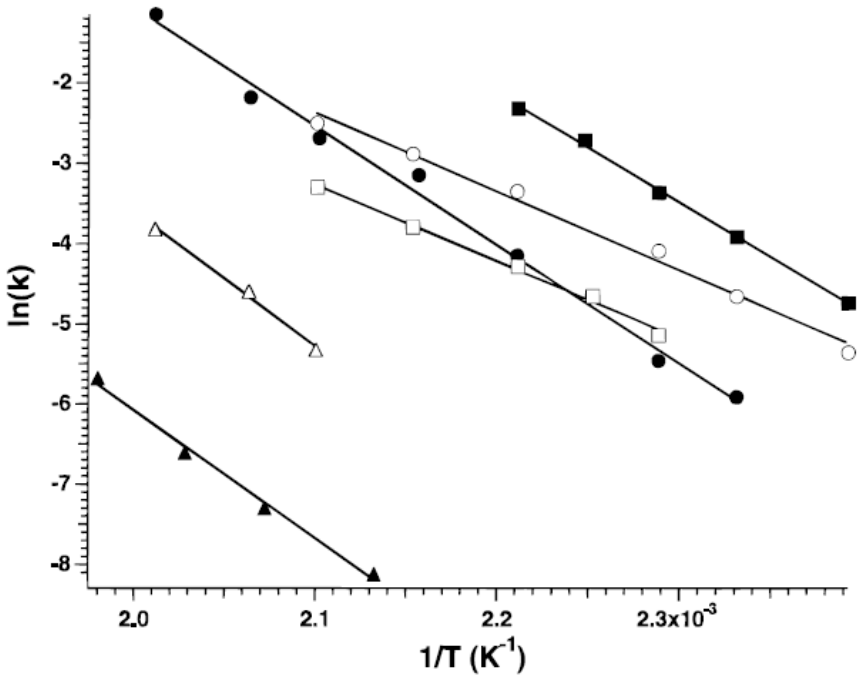


Figure 6

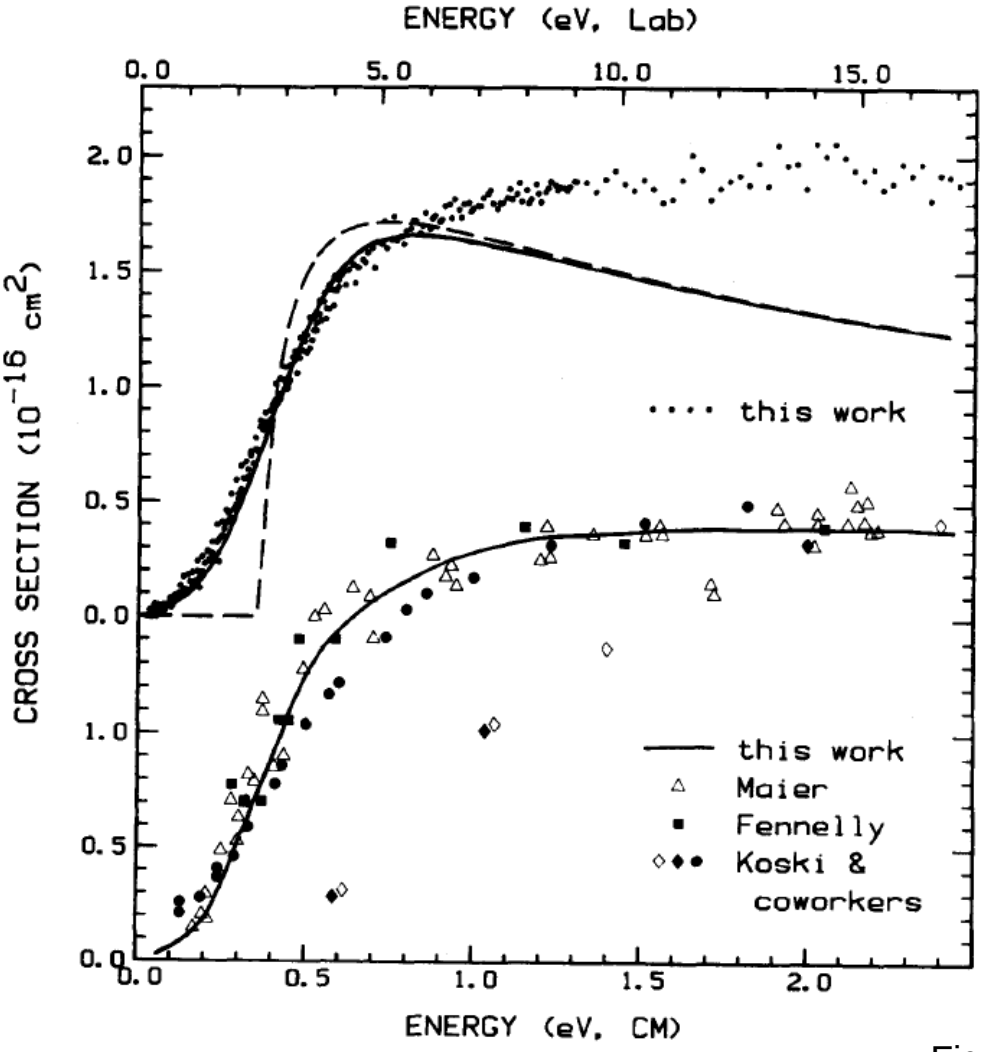


Figure 7

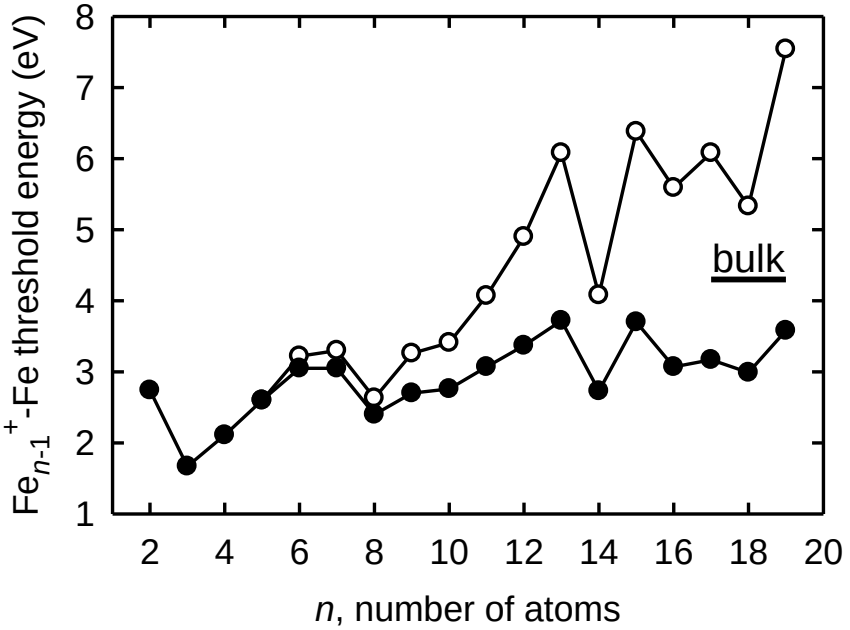


Figure 8

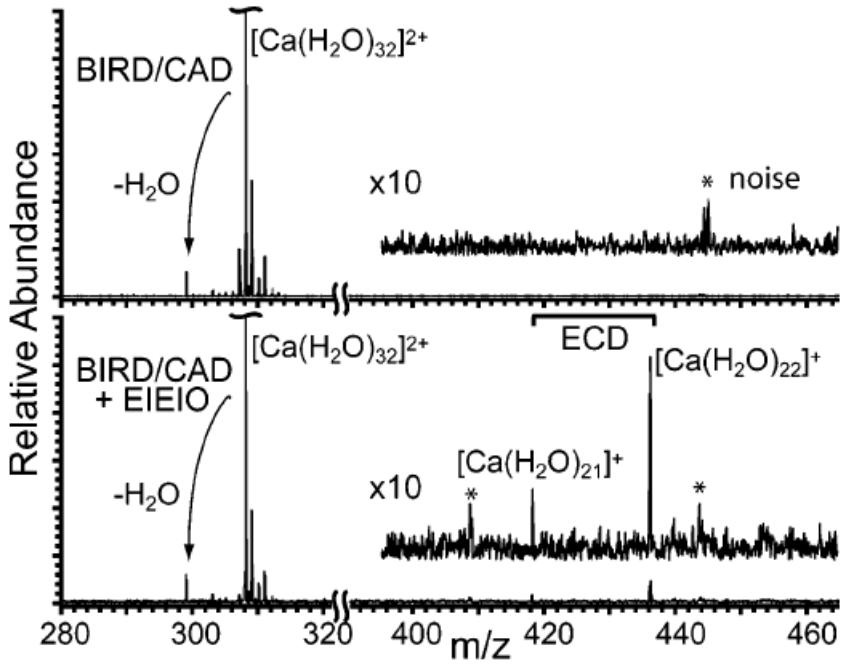


Figure 9

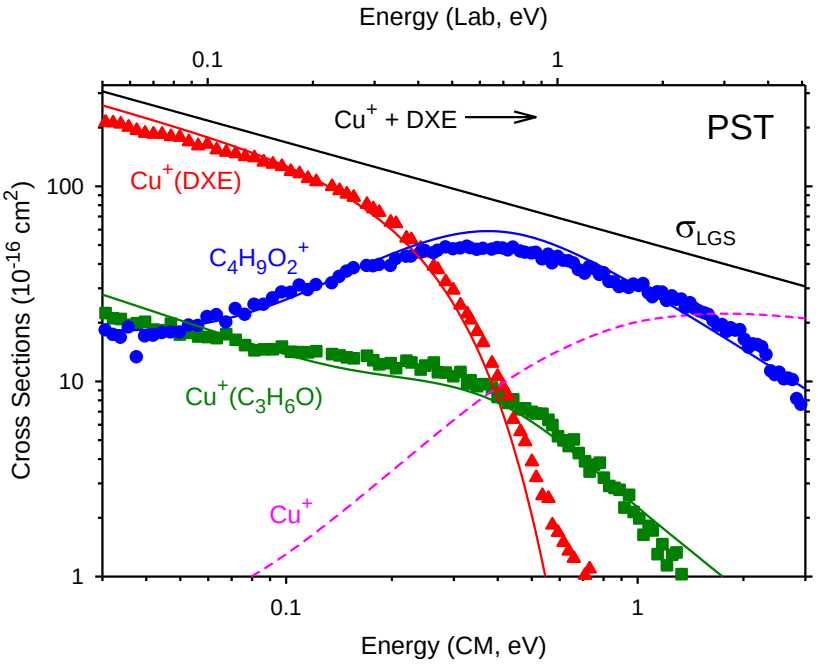


Figure 10